Journal of Aeronautics, Astronautics and Aviation, Vol. 56, No. 1S, pp. 469 – 476 (2024)
DOI: https://doi.org/10.6125/JoAAA.202403_56(1S).34

Performance of DOA Estimation Algorithms for Acoustic Localization of Indoor Flying Drones Using Artificial Sound Source

Syaril Azrad [1, 3] *, Abdulaziz Salman [1], Syed Abdul Rahman Al-Haddad [2]

[1]*Department of Aerospace Engineering, Faculty of Engineering, Universiti Putra Malaysia, 43400 Serdang, Selangor, Malaysia*
[2]*Department of Computer and Communication Systems Engineering, Faculty of Engineering, Universiti Putra Malaysia, 43400 Serdang, Selangor, Malaysia*
[3]*Aerospace Malaysia Research Center, Universiti Putra Malaysia, 43400 Serdang, Selangor, Malaysia*

ABSTRACT

Flying unmanned aerial vehicles (UAVs) in swarms can have numerous advantages. However, to maintain a safe distance between them during flight is very challenging. To achieve this, each UAV in the swarms needs to know its relative location with respect to one another. This work proposes a method for relative localization using the chirping sound emitted from UAVs flying together indoors. The strategy is simulated to assess localization performance of three different types of chirping sounds indoors using six microphone arrays. The estimated direction of arrival (DOA) of the chirping sound is calculated using several published algorithms that include MUSIC, CSSM, SRP-PHAT, TOPS and WAVES. The sound is produced in a simulated flying indoor environment with several different settings of sound-to-noise ratio (SNR) and reverberation time (RT). Based on the results, it has been found that chirping sound with a wider frequency band produced better results in terms of mean values of DOA estimation error. The chirping sound performance is also tested with the actual UAVs operating under different rotor speeds. Similarly, it is observed that the chirping sound with wider band also produced better results in three of the algorithms, which is reflected in their absolute mean error. Nevertheless, further work has to be done to filter out the UAVs' rotor noise and also the indoor reverberation effects for better performance.

Keywords: Aerial robotics, Swarms, Localization, Acoustic signaling

I. INTRODUCTION

In general, unmanned aerial vehicles (UAVs) are the category of aerial vehicles that are able to take off and land without the need for onboard pilot, and they can be either controlled remotely or autonomously [1]. To date, the use of UAVs has gained increasing popularity because of the capabilities they offer. Among others, these flying robots are capable of giving high-view sensing of target locations and can quickly reach areas of interest by flying over barriers and inaccessible terrains. Examples of current applications for UAVs include agricultural crop spraying [2], military reconnaissance [3], aerial photography [4], remote sensing and land mapping [5], and package delivery [6]. In the meantime, for certain missions such as exploration, search and rescue, and surveillance, the resiliency and efficiency of such operations could be improved through redundancy, parallelism and collaboration of a team of UAVs instead of a single flying UAV [7]. This is because swarming UAVs can create a larger exposed area. Nevertheless, it should be noted that having a team of flying UAVs can also increase the risk of collision, especially intra-swarm collision since they fly in

Manuscript received, October 20, 2023, final revision, December 13, 2023
* To whom correspondence should be addressed, E-mail: syaril@upm.edu.my

close proximity to each other [8]. Therefore, it is vital to have an accurate position of each UAV in the swarm.

To achieve the avoidance collision system, obtaining the relative positioning information of the other UAVs is a key element [9]. At this moment, several systems, such as global positioning systems (GPS) [10] and vision sensors [11], are planted into UAVs' swarms in order to achieve accurate avoidance of collision. However, these systems are greatly dependent on other external systems. For instance, GPS is a triangular-based satellite positioning that may be unsuitable for application in indoor or GPS-denied areas due to signal loss. Meanwhile, it can be noted that commercial aircraft are relatively positioned in the sky using radar-based technologies such as the Traffic Collision Avoidance System (TCAS) [12]. While TCAS works well for aircraft, it is too expensive and cumbersome for UAVs' applications. Alternatively, it is proposed to use sound-based sensors on UAVs, especially for swarming UAVs, which is believed to be the effective solution for the aforementioned issues in collision avoidance purposes.

The development of a localization system for relative positioning or localizing a desired sound is gaining interest among the research community. For instance, a study has been conducted on localizing the sound of emergency whistles for search and rescue operations. In this particular study, a particle filter is used to combine data from the cross-correlation of signals obtained by four spatially separated microphones installed on the micro aerial vehicle (MAV), the dynamics of the aerial platform and the frequency shift caused by the MAV's mobility [13]. Furthermore, researchers use different localization algorithms to find the target DOA. One of them is MUltiple SIgnal Classification (MUSIC), which is a DOA method that uses second-order statistics to approximate the spatial spectrum by using the eigenspace of the source signals and noises [14].

Another subspace method, the Coherent Signal-Subspace Method (CSSM), aims to create a single signal subspace that allows for high-resolution estimates of the angles at which several wideband plane waves [15]. Additionally, other algorithms that have been used include Weighted Average of Signal Subspaces (WAVES), which is formulated to construct an improved design of focusing matrices on guaranteeing a statistically sound preprocessing of wideband data [16], and Test of Orthogonality of Projected Subspaces (TOPS), which is another coherent technique for wideband signals and works by measuring orthogonal relationship between the signals and the noise subspaces of various frequency components of the sources to obtain the approximate DOA [15]. Last but not least, the Steered-Response Power Phase Transform (SRP-PHAT) is a well-liked localization method for locating acoustic sources, and it is known for its steadfast performance in challenging acoustic conditions. In brief, this algorithm is based on beamforming and seeks out the candidate position that increases the output of the steered delay-and-sum beamforming [17]. It should be noted that, based on available works of literature, there is yet to be any attempt to use the aforementioned localization system algorithms in the UAV swarm technique.

In conjunction with this notion, the research work done in this study investigates the performance of the direction of arrival (DOA) localization algorithms to obtain the relative positioning of another drone based on the UAV's ego-noise in a swarm of UAVs. In short, the UAV's ego-noise is defined as the generated noise by the motors and propellers of the UAV [18]. Furthermore, the algorithms are also tested with different artificial chirping sounds. It is suggested that the chirping sound be applied as a strategy for sound-based localization of the UAVs in swarms for collision avoidance, which follows the research work by Basiri et al. [9].

II. SETUP AND METHODOLOGY

2.1 Algorithms Applied

For this study, several algorithms are used to estimate DOA with different base techniques, including time delay, subspace and beamforming. Time Difference of Arrival or TDOA is a method to find the direction of the signal source by using the time delay, τ_n, between sensors. It is formed in the geometrical formula in Equation (1), where d is the distance between microphones while c is the speed of sound [19].

$$\theta_n = \arcsin\left(\frac{\tau_n c}{d}\right) \tag{1}$$

The DOA of the received source can be obtained from the subspace MUSIC, which is provided by Equation (1) and Equation (2). This exploits the independence of both signal source and noise, and maximizes the pseudo-spectrum of all DOA candidates.

$$\hat{P}_{MUSIC}(\mathbf{e}(\theta)) = \frac{1}{\sum_{i=p+1}^{N} |\mathbf{e}(\theta)^H \mathbf{v}_i|} \tag{2}$$

$$\hat{\theta} = \operatorname{argmax}_\theta \hat{P}_{MUSIC}(\theta) \tag{3}$$

Both the noise eigenvectors, $\mathbf{v}$ and candidate steering vector, $\mathbf{e}(\theta)$ have a property of orthogonality [16], and this can be rewritten in the STFT domain to find the DOA by summing all k frequency bins as in Equation (4). Moreover, to avoid a low magnitude participation due to the variation of magnitude in the frequency bins, it is normalized by dividing it with the maximum MUSIC pseudo-spectra per frequency bin, which is given in Equation (5). This leads to the normalized MUSIC that is presented by Equation (6) and Equation (7).

$$\tilde{P}_{MUSIC}(\theta) = \sum_{k=1}^{K} \hat{P}_{MUSIC}(\theta, k) \tag{4}$$

$$\hat{\theta}_k = \max_\theta \hat{P}_{\text{MUSIC}}(\theta, k) \tag{5}$$

$$\hat{P}_{\text{NormMUSIC}}(\theta,k) = \frac{\hat{P}_{MUSIC}(\theta,k)}{\hat{\theta}_k} \quad (6)$$

$$\tilde{P}_{\text{NormMUSIC}}(\theta) = \sum_{k=1}^{K} \hat{P}_{\text{NormMUSIC}}(\theta,k) \quad (7)$$

Meanwhile, CSSM is another subspace algorithm for wideband sources using a transformation matrix (focusing matrix) that is dependent on the frequency bins. It merges correlation matrices at various frequency bins into a single correlation matrix, $\mathbf{R}_{\text{gen}}$, at one focusing frequency. This is as denoted by Equation (8), where H is a conjugate transpose, $\mathbf{T}_i$ is focusing matrices of frequency i = 1,..,K-1, reference frequency focusing metrics $\mathbf{T}_0$ = I, α_i is the weighting, and $\mathbf{Q}_i$ is the correlation matrix of the estimated narrowband. This process is known as concentrating. In case of finding the DOA, MUSIC can be used after converting wideband into narrowband

$$\mathbf{R}_{\text{gen}} = \sum_{i=0}^{K-1} \alpha_i \mathbf{T}_i \mathbf{Q}_i \mathbf{T}_i^H \quad (8)$$

On the other hand, the previous method is changed a bit into WAVES by using the weighted signal subspaces of Equation (9), whereby $\mathbf{F}_i$ is the signal subspace and $\mathbf{P}_i$ is the weighting matrix of frequency, w_i.

$$\mathbf{Q}_i = \mathbf{F}_i \mathbf{P}_i \mathbf{P}_i^H \mathbf{F}_i^H \quad (9)$$

In addition, orthogonality test between the modified signal subspace and the noise subspace is carried out by TOPS. The method uses transformation matrix in Equation (10) at each hypothesized DOA, and orthogonality is retained when the hypothesized DOA matches the real DOA. The transformation matrix in Equation (10) is applied to map an array manifold $\mathbf{a}_i$ (θ_i) to a new array manifold $\mathbf{a}_k$ (θ_k), and j is identical sized block from the sensor output. Equation (11) shows the new array manifold $\mathbf{a}_k$ (θ_k), whereby $\mathbf{a}_i$ (θ_i) is a function of two parameters: bin frequency and DOA $\mathbf{a}(\omega_i,\theta_j)$ M×1 from steering matrix $\mathbf{A}(\omega_i,\theta)$. The estimated DOA can be obtained from Equation (12), and it is dependent on hypothesized angle. This matrix contains the smallest singular value, σ_{min} (ϕ).

$$[\Phi(\omega_i,\theta_i)]_{(k,k)} = \mathrm{e}^{(-j\omega_i v_k \sin\theta_i)} \quad (10)$$

$$\mathbf{a}_k(\theta_k) = \mathbf{\Phi}(\omega_j,\theta_j)\mathbf{a}_i(\theta_i) \quad (11)$$

$$\hat{\theta} = \arg\max_{\phi} \frac{1}{\sigma_{min}(\phi)} \quad (12)$$

SRP-PHAT is based on beamforming to search for the steer direction with the highest power in delay-and-sum beamformer. The steered response of k discrete temporal frequency and continuous steering, $\Delta_1 \ldots \Delta_M$, delays can be represented as Discrete Fourier Transform (DFT), which is given in Equation (13). In this equation, $X_{\text{m,b}}[k]$ represents microphone M signals in each DFT block b, and $G_{m,b}[k]$ is a discrete-time filter. Furthermore, the steered response power is obtained by summing over K, as in Equation (14). This equation is reformatted in terms of PHAT, as shown in Equation (15), to form the final SRP-PHAT

$$\tilde{Y}_{\zeta}(k,\Delta_1 \ldots \Delta_M) \equiv \sum_{m=1}^{M} G_{m,b}[k] X_{m,b}[k] e^{-j\omega\Delta_m} \quad (13)$$

$$\tilde{P}_b(\Delta_1 \ldots \Delta_M) \equiv \sum_{k=1}^{K} \tilde{Y}_b[k,\Delta_1 \ldots \Delta_M)\tilde{Y}_b'[k,\Delta_1 \ldots \Delta_M) \quad (14)$$

$$\tilde{P}_b^{PHAT}(\Delta_1 \ldots \Delta_M) \equiv \sum_{k=1}^{K} \tilde{Y}_b^{PHAT}[k,\Delta_1 \ldots \Delta_M)\tilde{Y}_b^{'PHAT}[k,\Delta_1 \ldots \Delta_M) \quad (15)$$

2.2Simulation Setup

All of the above algorithms are implemented by using Pyroomacoustics Python library. This library contains a few pre-built localization algorithms with parameters that have been pre-defined by several previous researchers [20]. The algorithms are built considering near field with a sound frame of 1024 and a frequency sample of 44,100. These algorithms have received a signal in the form of Short Time Fourier Transform (STFT) with 50% overlap. It provides the simulation setup to produce sounds inside a simulated room, which is accomplished by creating a Room Impulse Response (RIR) with two different methods: Image Source Method (ISM) and Ray Tracing. This capability aids in minimizing the labor time that is otherwise needed to design the optimal distinguishing signal sound source to reduce the localization error.

The simulation is run for 100 random positions for the algorithms using three different types of chirping sounds in two different stages. The first stage is with varying sound-to-noise ratio (SNR) levels at reverberation time (RT) of 0.4 s while the other one is with varying RT and pure signals (no SNR is added).

2.3 Experimental Setup

The experiments have been implemented using two hobby UAVs (i.e. leader and follower) mounted on tripods. Both of the UAVs are similar in terms of their components, their propellers are 1045 with brushless motors of 1000 Kv and they are controlled by using the flight microcontroller Betaflight F4v3s.

For the experiment, as shown in Figure 1, the follower UAV is placed away from the leader drone at five different positions. Both UAVs have been equipped with reflective markers, which are detected by OptiTrack motion capture system to determine their exact positions.

As can be observed in Figure 1, the leader is placed at the center of the room, and it has been equipped with a six-microphones recording device (ReSpeaker 6). The details of this recording device are listed in Table 1. The

recording device module is raised by 15 cm from the UAV's upper-center frame part to reduce the effects of mechanical ego-noise contributed mainly by the spinning rotors of the UAV.

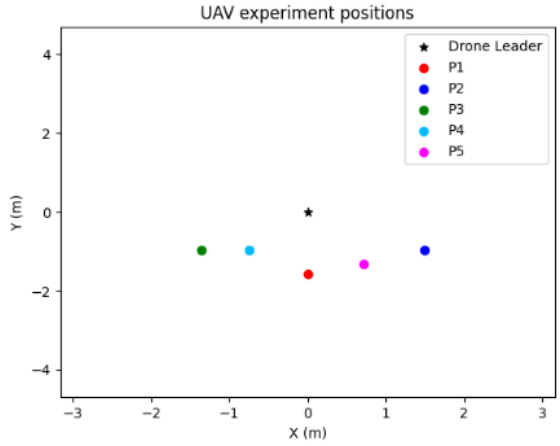

Figure 1 Positions of the UAVs in the room

Table 1 Microphone array specification

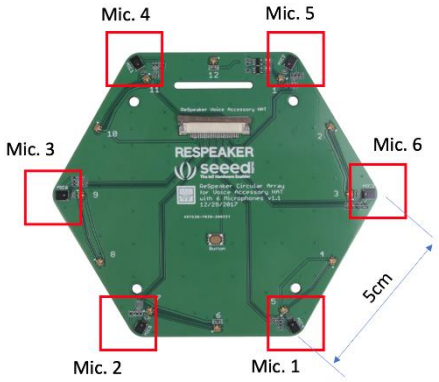

Specification	Value
Name	ReSpeaker 6
Number of Microphone	6
Sensitivity	-22 dBFS (Omnidirectional)
SNR	59 dB
Maximum Sample Rate	48 kHz
Recording Program	Audacity 3.1
Dimension	Hexagonal with side length of 5 cm

The data are taken with different speeds of each UAV in the five aforementioned positions. The speeds used are 0 rpm, 1250 rpm, 1350 rpm and 1450 rpm. In this case, the speed of the leader UAV is varied at these four different levels and at each level, the speed of the follower UAV is varied at three different levels (i.e. without 0 rpm) for each of the considered positions. Hence, at each of the five different positions for the follower UAV, there are 12 different combinations of speed with the leader UAV. Furthermore, the collected data is taken at three different stages.

In the first stage, the collected data is just due to the propellers of both UAVs. This process is called passive method, where localization is based solely on UAVs' mechanical sounds. On the other hand, three different artificial sources of the chirping sound are used, which is the active method where the DOA estimation of the follower UAV from the location of the leader UAV is assisted by additional cues from the follower UAV. The three artificial chirping sounds used in simulation and experiments are designed for narrowband with high frequency, chirping sound designed to meet the characteristic in Equation (16) and lastly, a stacked chirping sound with a wider band.

For the second chirping sound, the frequency is tuned based on Equation (16), which states that the speed of sound, c divided by the double of center frequency of the bandwidth, f_0, should be larger than the distance between two microphones, d_m, in order to make a peak difference in cross-correlation to obtain TDOA [21]. From the results of the two chirping sounds, it is found that the number of frequency bins affects the DOA estimation results. The third chirping sound is designed by stacking ten chirping sounds of 1 kHz to create a wider band that contains multiple frequency bins and hence contains more information. The experimental settings for the passive and active methods are respectively summarized in Table 2 and Table 3. Refer to Figure 1 for the P1-P5 follower locations.

$$d_m < \frac{c}{2f_0} \tag{16}$$

Table 2 Passive method experimental settings

Leader (rpm)	Follower (rpm)	Follower Location
0	1250, 1350,1450	P1-P5
1250	1250, 1350,1450	P1-P5
1350	1250, 1350,1450	P1-P5
1450	1250, 1350,1450	P1-P5

Table 3 Active method experimental settings

Leader (rpm)	Follower (rpm)	Follower Location	Chirping Sound	DOA Algorithm
0	1250, 1350,1450	P1-P5	Type 1, 2, 3	NormMUSIC, CSSM, SRP-PHAT, TOPS, WAVES
1250	1250, 1350,1450	P1-P5	Type 1, 2, 3	
1350	1250, 1350,1450	P1-P5	Type 1, 2, 3	
1450	1250, 1350,1450	P1-P5	Type 1, 2, 3	

III. RESULTS AND DISCUSSION

3.1 Simulation Results

Three different types of chirping sounds are used in the simulation that is implemented with Pyroomacoustics Python library. In this experiment, three different chirping frequency range settings are applied, which are between 6 to 8 kHz, 0.5 to 2.330 kHz and combined chirping sound from 0.020 to 10 kHz with a single chirping sound each 1 kHz. All sounds are played in a room with dimensions of 6.32 m width, 9.37 m length and 3.31 m height, with two changing parameters that are SNR and RT. Figure 2 shows the localization results of high-frequency chirping sound using all five algorithms with the two parameters varied from -25 to 25 for SNR and 0.2 to 2.0 for RT. The results have shown that the errors are below 10° for various RTs for all algorithms except for CSSM. However, this type of chirping sound did not produce good results even with low SNRs. This can be attributed to the lack of information on the frequency bins of the sound source, which eventually affects overall DOA estimation, as reflected in the results.

Meanwhile, the chirping sound designed by considering Equation (16) has outperformed the previous sound source in low SNRs, showing very stable localization results as depicted in Figure 3 for four of the five algorithms applied. This designed sound is taken as a wideband sound source, consisting of large amounts of information in the STFT domain, so all algorithms perform well in low SNR except TOPS, where the error is huge. For varying RTs, the wideband shows its sensitivity to RT as it increases.

Lastly, all algorithms perform better for the combined or stacked multi-chirping sounds of 1 kHz to 10 kHz, which is designed to provide more information in the frequency bins, which can be observed in Figure 4. All algorithms are performing much better than high-frequency chirping sound in low SNRs, where the results are almost stable at -15 dB SNR. Additionally, it could be observed that the resistance of RT has also improved and is much better than that for the designed chirping sound.

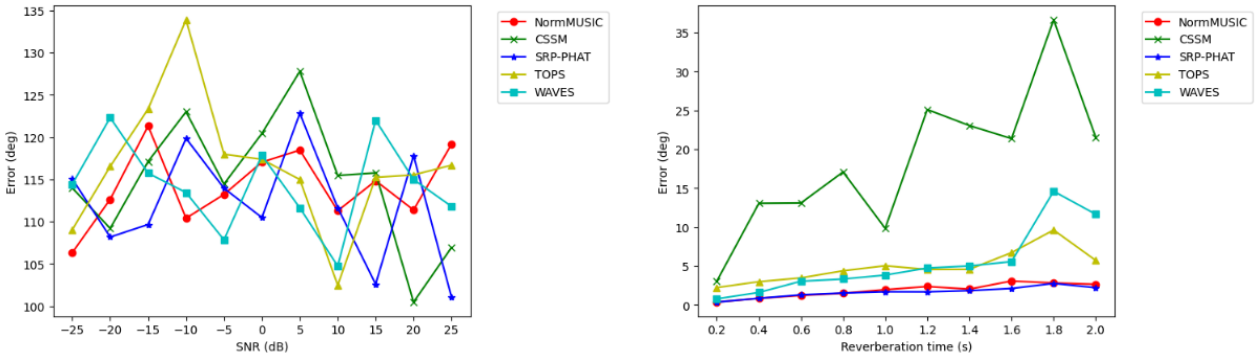

(a) With varying SNR (b) With varying RT

Figure 2 DOA estimation results for high-frequency, narrow-bin chirping sound

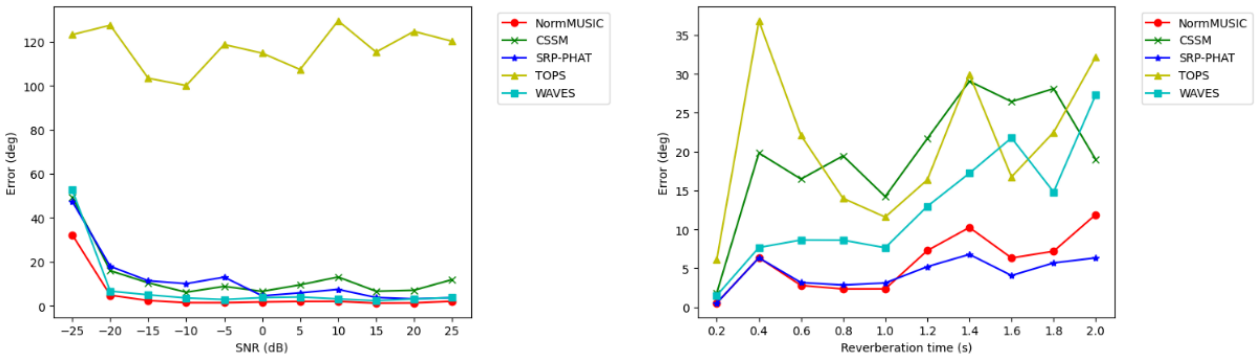

(a) With varying SNR (b) With varying RT

Figure 3 DOA estimation results for designed chirping sound

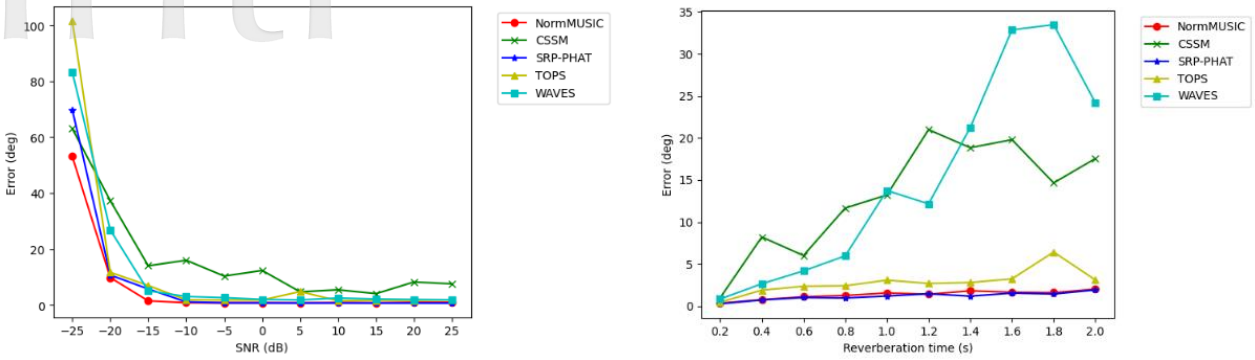

(a) With varying SNR (b) With varying RT

Figure 4 DOA estimation results of combined (stacked) chirping sound

3.2 Experimental Results

The experiments have been conducted in four stages of chirping sounds, as examined in the previous simulation with sounds of propellers and motors. Figure 5 to Figure 8 show the results of the different localization algorithms for Position 1 of the follower UAV with a true angle degree of 270°. The x-axis is arranged in terms of increasing sum of the rotor speed for both leader and follower UAVs. The left end of the axis is when the leader or/and follower UAVs' rotors are not spinning (0 rpm), while the right end of the axis is where both the leader and follower UAVs' rotors are operated at a maximum speed of 1450 rpm. The UAVs' sound consists of both wideband and narrowband, and it has a frequency range based on the speed of the motors.

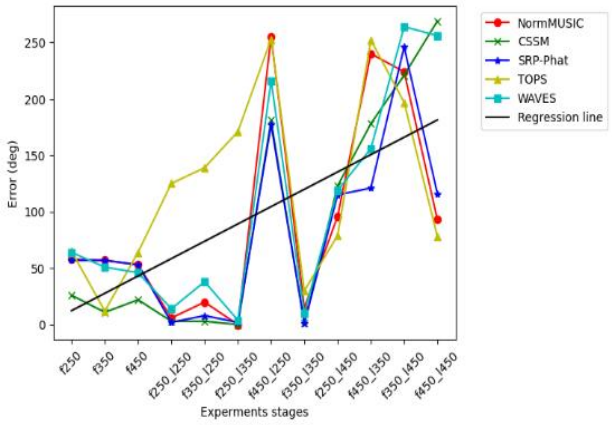

Figure 5 DOA estimation results at Position 1 of follower UAV with just ego-noise

Figure 5 depicts the localization system of just using ego-noise of the follower UAV, and all algorithms perform quite well when the follower UAV is at high speed while the leader UAV's rotor is not operating or operating at low speed. This could be attributed to the fact that when the leader UAV is operated at a lower speed, interferences from its rotors are lesser, and information used by the algorithms is predominantly based on information from follower UAV's motors and propellers. The mechanical sound of follower UAV contains a wider range of frequency bins that leads to better localization estimation results. As anticipated, the DOA estimation algorithms results are erroneous when the leader UAV's ego noise is increased. This is shown clearly in the regression line, which represents the error degree in all experiment stages, and it is a positive correlation to the variation of motor speed.

Meanwhile, Figure 6 and Figure 7 show the estimated DOA results in the case of the high-frequency, narrow-bin chirping sound and the designed chirping sound. It can be observed that the obtained results from all algorithms for both situations are not good. The main reason for this can be attributed to the high ego noise from the UAVs and the high RT generated in the room. In general, for the case of high-frequency, narrow-bin chirping sound, the error appears to increase with increasing speed of leader and/or follower UAVs. This general finding is in contrast to the designed chirping sound, as the error seems to lessen with increasing speed. As for the combined (stacked) chirping sound, the mean value of the error from all algorithms appears to be rather constant with the increasing speed of the UAVs, which is depicted in Figure 8.

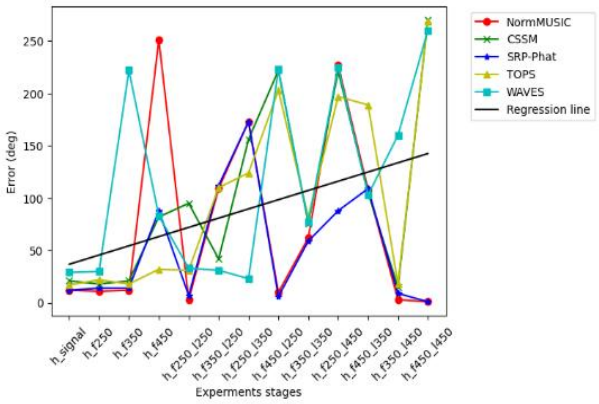

Figure 6 DOA estimation results at Position 1 of follower UAV with high-frequency, narrow-bin chirping sound

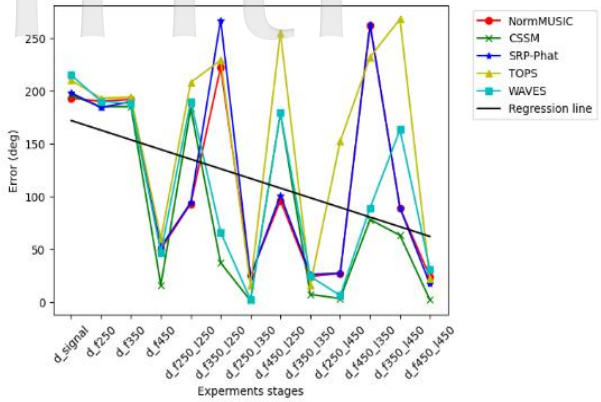

Figure 7 DOA estimation results at Position 1 of follower UAV with designed chirping sound

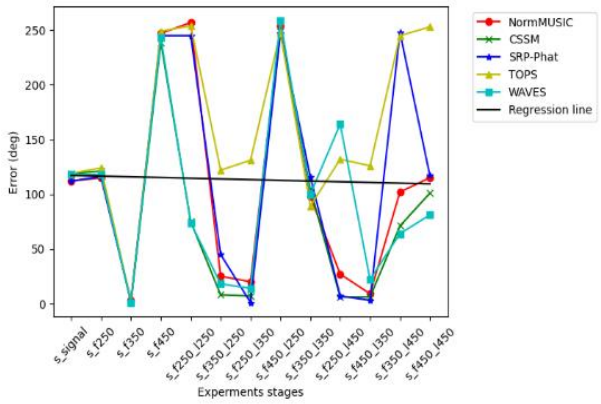

Figure 8 DOA estimation results at Position 1 of follower UAV with combined (stacked) chirping sound

Overall, Figure 9 summarizes the performance of all considered algorithms according to their absolute mean error for each of the four stages of the chirping sound. It can be observed that the combined chirping sound has performed better among all of the sound types for three of the algorithms, with the exception of the SRP-PHAT and TOPS algorithms. Note that this type of sound has the main drawback of having difficulty with filtration.

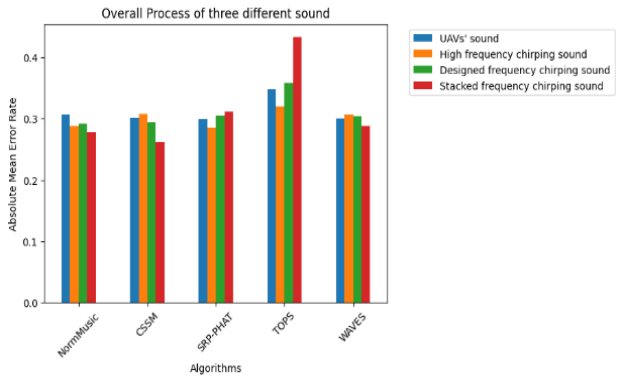

Figure 9 Mean absolute error of all five positions

IV. CONCLUSIONS

For sound-based localization of UAVs in a swarm, the use of motors and propellers as the sources for the sound is good. However, the primary drawback is the disturbance from the leader UAV's mounted microphone. To resolve this issue, it has been suggested that chirping sounds are to be used to determine the relative positioning of the UAVs. Based on the results of this study, it has been found that using the chirping sounds without an anti-reverberation filter inside the room has led to low accuracy of localization algorithms. Some algorithms, such as CSSM, are more suitable for wideband sound localization, which shows the drawback of attempting to localize in high RT. The indoor environment suffers from signal reflection due to the high noise produced by the motors and propellers of UAVs. Thus, the application of manual localization techniques becomes tedious in such an environment. In future works, Deep Learning (DL) models can be studied as an auto feature extractor to accomplish the task of UAV localization with very minimal manual extraction, which has witnessed some remarkable results in multiple works of research on speech localization. In addition, an optimized chirping sound can be designed to improve the localization system.

ACKNOWLEDGMENTS

The authors acknowledge the support for this study by Ministry of Education, Malaysia, through Fundamental Research Grant Scheme: FRGS/1/2020/TK0/UPM/02/33.

REFERENCES

[1] Chen H, Wang XM, Li Y, "A survey of autonomous control for UAV," Proceedings of the International Conference on Artificial Intelligence and Computational Intelligence, 2009.

[2] Nasir RE, Hamdan HA, Hamid AHA, Mohamed WMW, Sapak Z, "Development of crop-spraying module for multirotor drone," *Journal of Aeronautics, Astronautics and Aviation*, Vol. 54, No. 3, 2022, pp. 315-324.

[3] Wang Y, Bai P, Liang X, Wang W, Zhang J, Fu Q, "Reconnaissance mission conducted by UAV swarms based on distributed PSO path planning algorithms," *IEEE Access*, Vol. 7, 2019, pp. 105086-105099.

[4] Liu H, Lin M, Deng L, "UAV route planning for aerial photography under interval uncertainties," *Optik*, Vol. 127, No. 20, 2016, pp. 9695-9700.

[5] Everaerts J, "The use of unmanned aerial vehicles (UAVs) for remote sensing and mapping," *The International Archives of the Photogrammetry, Remote Sensing and Spatial Information Sciences*, Vol. 37, 2008, pp. 1187-1192.

[6] Lin CE, Li CC, Shao PC, Luo CF, "Precision UAV parcel delivery using QR code recognition," *Journal of Aeronautics, Astronautics and Aviation*, Vol. 51, No. 3, 2019, pp. 275-289.

[7] Bahiki MR, Talib NNA, Azrad S, "Relative positioning-based system with tau control for collision avoidance in swarming application," *IOP Conference Series: Materials Science and Engineering*, Vol. 152, No. 1, 2016, 012025.
[8] Yaghoobi Y, Bahiki MR, Azrad S, "Feature-based stereo vision relative positioning strategy for formation control of unmanned aerial vehicles," *International Journal of Innovative Technology and Exploring Engineering*, Vol. 9, No. 2, 2019, pp. 1613-1617.
[9] Basiri M, Schill F, Lima P, Floreano D, "Onboard relative bearing estimation for teams of drones using sound," *IEEE Robotics and Automation Letters*, Vol. 1, No. 2, 2016, pp. 820-827.
[10] Vetrella AR, Fasano G, "Cooperative UAV navigation under nominal GPS coverage and in GPS-challenging environments," Proceedings of the IEEE 2nd International Forum on Research and Technologies for Society and Industry Leveraging a Better Tomorrow, 2016.
[11] Cheong MK, Bahiki MR, Azrad S, "Development of collision avoidance system for useful UAV applications using image sensors with laser transmitter," *IOP Conference Series: Materials Science and Engineering*, Vol. 152, No. 1, 2016, 012026.
[12] Romli F, King J, Li L, Clarke JP, "Impact of automatic dependent surveillance-broadcast (ADS-B) on traffic alert and collision avoidance system (TCAS) performance," Proceedings of the AIAA Guidance, Navigation and Control Conference and Exhibit, 2008.
[13] Yamada T, Itoyama K, Nishida K, Nakadai K, "Sound source tracking using integrated direction likelihood for drones with microphone arrays," Proceedings of the IEEE/SICE International Symposium on System Integration, 2021.
[14] Salvati D, Drioli C, Foresti GL, "Incoherent frequency fusion for broadband steered response power algorithms in noisy environments," *IEEE Signal Processing Letters*, Vol. 21, No. 5, 2014, pp. 581-585.
[15] Yoon YS, Kaplan LM, McClellan JH, "TOPS: New DOA estimator for wideband signals," *IEEE Transactions on Signal Processing*, Vol. 54, No. 6, 2006, pp. 1977-1989.
[16] Di Claudio ED, Parisi R, "WAVES: Weighted average of signal subspaces for robust wideband direction finding," *IEEE Transactions on Signal Processing*, Vol. 49, No. 10, 2001, pp. 2179-2191.
[17] Cai W, Zhao X, Wu Z, "Localization of multiple speech sources based on sub-band steered response power," Proceedings of International Conference on Electrical and Control Engineering, 2010.
[18] Insausti X, Hogstad BO, Pätzold M, "Modelling and simulation of ego-noise of unmanned aerial vehicles," Proceedings of the IEEE 91st Vehicular Technology Conference, 2020.
[19] Jahana CJ, Sinith MS, Lalu PP, "Direction Of Arrival Estimation using Microphone Array," Proceedings of the Fourth International Conference on Microelectronics, Signals & Systems (ICMSS) IEEE, 2021.
[20] Scheibler R, Bezzam E, Dokmanić I, "Pyroomacoustics: A python package for audio room simulation and array processing algorithms," Proceedings of the IEEE International Conference on Acoustics, Speech and Signal Processing, 2018.
[21] Djurek I, Petosic A, Grubesa S, Suhanek M, "Analysis of a quadcopter's acoustic signature in different flight regimes," *IEEE Access*, Vol. 8, 2020, pp. 10662-10670.